Free Surface Detection in Hydraulic Jumps through Image Analysis and Ultrasonic Sensor Measurements

J.D. Nóbrega[1] , H.E. Schulz[1] and D.Z. Zhu[2]
[1]School of Engineering of São Carlos
University of São Paulo
São Carlos, SP, 13566-590
BRAZIL
[2]Dept. of Civil and Environmental Engineering, University of Alberta
Edmonton, Alberta, T6G 2W2
CANADA
E-mail: junobreg@gmail.com

Abstract: *The application of non-intrusive techniques has been sought in experimental studies involving complex hydraulic phenomena. In this sense, in the present study an ultrasonic sensor and a high speed camera were used for measurements in hydraulic jumps, in order to evaluate the free-surface characteristics. The free surface was identified in the images using relatively simple procedures of image processing. The proposed methodology for image analysis is relatively robust and produces the mean longitudinal interface profile compatible to that obtained with the ultrasonic sensor. The results of the present study include mean free surface profile, time evolution of the free surface and toe oscillation.*

Keywords: *hydraulic jumps; image processing; free surface profile; non-intrusive techniques.*

1. INTRODUCTION

A hydraulic jump is a complex phenomenon that occurs when a supercritical flow changes suddenly to a subcritical flow. The water surface initially rises abruptly at the toe of the jump, continuing to rise more softly along the flow, until the subcritical sequent depth is attained. Downstream of the position where the hydraulic jump sets in, a recirculation region forms above a bottom jet in expansion, presenting a superficial flow opposite to the main flow direction. While the most common type of hydraulic jump occurs in open channels, it can also be observed in circular pipes and in stratified flow conditions. The hydraulic jump formed in open channel with parallel walls and horizontal bottom is called the classical or type *A* hydraulic jump, which is the focus of the present paper (Rajaratnam, 1995).

Because of the high energy dissipation and significant air entrainment that occurs in hydraulic jumps, its research has a major importance in the design of hydraulic structures. Though hydraulic jumps have been studied for a long period, many of their internal characteristics are not completely understood due to the unsteady and three-dimensional nature of the jump. In this sense, the study of the free surface position may contribute to the knowledge of the internal structure of the flow, which is composed by large-scale eddies that interact with the free surface (Long *et al,* 1991).

A particular characteristic of hydraulic jump is the large amount of entrapped air in the flow. Air bubbles are introduced mainly at the region of impact between the high velocity bottom jet and the roller, being then conducted to an intermediate layer in the hydraulic jump (Chanson, 2009). The void fraction is also affected by the air-water interactions, as the collapse of the free surface leads to local air entrainment (Rodríguez-Rodríguez *et al*, 2011).

In more recent studies non-intrusive techniques were used for locating the interface in stepped spillways, as shown, for example, by Bung (2013), who used ultrasonic sensors and a high speed camera. Studies of the air-water interface in stepped channels using ultrasonic sensors presented good results for different relevant parameters in such flows, as the position of the inception point for aeration, the transition length for complete aeration, among other parameters, as shown by Simões *et al* (2011 a, b, 2013). Authors like Murzyn *et al* (2007), Kucukali & Chanson (2008), Murzyn & Chanson (2009 a, b), Chachereau & Chanson (2010, 2011) investigated the dynamics of the air-water interface

in hydraulic jumps combining different methodologies. The first authors used wire gauges while the others performed the measurements with acoustic displacement meters in conjunction with phase detection probes.

Regarding to image analysis, some researchers have used PIV (Particle Image Velocimetry) and BIV (Bubble Image Velocimetry) techniques for determining the instantaneous velocity flow field (Misra *et al*, 2008; Bung, 2011; Rodríguez-Rodríguez *et al*, 2011; Lin *et al*, 2012). Studies on bottom aerators using combined techniques of PIV and Cesium 137 probe allowed obtaining very good void fraction profiles, used to quantify air entrainment along the water jet in such devices (Lima, 2004, Lima *et al*, 2008, 2009). Other authors have used different techniques of image processing, in order to acquire information directly from the images. Misra *et al* (2006), for example, estimated the air-water interface of a hydraulic jump through an image segmentation method, while Leandro *et al* (2012) developed an algorithm for determining the air concentration profile considering that the void fraction is related to the pixel intensities. These authors also determined the water surface time series based on a particular pixel intensity in the images.

The aim of the present study is to evaluate the evolution of the free surface of hydraulic jumps using ultrasonic sensors and a high speed camera, in order to contribute to the general comprehension of the flow structure in hydraulic jumps. In the following sections, the methodology proposed for image processing is presented, as well as the results of free-surface profile for a hydraulic jump with inflow Froude number of 2.39.

2. EXPERIMENTAL SETUP

The experiments were carried out in the Hydraulics Laboratory at the University of Alberta, Canada. The experimental apparatus consisted of a recirculation flume with plexiglass walls, having dimensions of 48 cm wide and 5 m long. The water was first discharged into a tank through a supply pipeline and then passed to the open channel through a plane gate (with a fixed opening of 25.4 mm), creating the supercritical condition. The flow rate was measured by a magnetic flow meter connected to the supply pipeline. The hydraulic jump position was controlled along the flume through a sluice gate located at the downstream end of the channel. For the purpose of this study, an ultrasonic sensor and a high speed camera were used, as described in detail in the items 2.1 and 2.2.The classical hydraulic jump was studied for an inflow Froude number (F_1) of 2.39 (Tab. 1). The jump toe was positioned 30 cm downstream of the sluice gate.

Table 1 – Experimental conditions.

Flow rate	Supercritical depth	Subcritical depth	Channel width	Supercritical velocity	Inflow Froude number
Q (Lps)	y_1 (mm)	y_2 (mm)	B (m)	U_1 (m/s)	F_1
Lps	Mm	mm	m	m/s	
16.00	27	80	0.48	1.23	**2.39**

2.1. High-speed camera

The images were taken with a high-speed camera (Phantom v211), positioned approximately 1.5 m from the flume sidewall. The region of interest of the flow was illuminated with a continuous laser sheet of 2.5 W (Stabilite 2017, Spectra-Physics Lasers), aligned with the central line of the flume. The images were recorded at a sample rate of 200 frames per second, resolution of 1024x512 pixels (21.3 pixels = 1 cm), generating a video with 5642 images in 28 s. A black board was placed in the backside of the flume, in order to reduce the blurring effects of the light diffraction caused by the bubbles in the aerated region.

The main challenge for the image processing was to adequately deal with the non-uniformity of the light intensity in the images. The causes of this non-uniformity were the different bubbles sizes and count rates, both in vertical and horizontal directions (Fig. 1). The mentioned problems, added to the fact that the contact of the water with the sidewall also generates a "shadow effect", affected the pixel

intensities of the water surface. In order to reference the observations to the position of the water surface, some steps were followed using the Image Processing Toolbox of Matlab® (Fig. 2).

The images were first cropped in frames with resolution of 313x1024 pixels, limiting the processing to the region of interest. The light diffraction caused by the air bubbles above the water surface, and also the bubbles attached to the glass wall (due to hydraulic jump movement and drop of water) are sources of noise for the automatic image processing. This noise was first minimized with the application of a mean filter, in which pixel intensities were replaced by mean pixel intensities based on a 3x3 neighborhood.
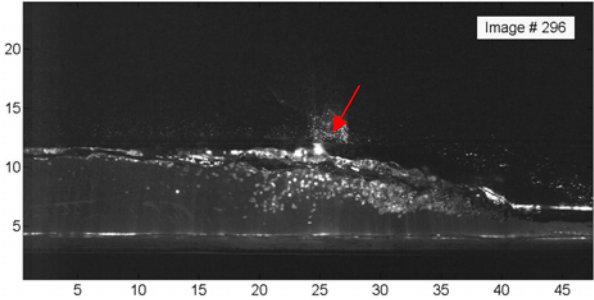

Figure 1 - Detail of the laser light diffraction caused by the bubbles and bubbles attached to the sidewall. *Image # 296* of the video. *Image scale*: centimetre.

After blurring the frames with the mean filter mask, the images were binarized. As the images present different pixel intensities, they were first subdivided in four regions with resolution of 313x256 pixels. For each region, a different threshold based on empirical observations was applied in order to preserve the free surface position. Even in the binarized images, some noise above the free surface could still be observed. Therefore, the pixel values were first replaced by the minimum pixel value found in a 3x3 neighborhood, and then by the maximum pixel intensity. The perimeter of the binary image was found with the function '*bwperim*' available on Matlab®, considering 8 connected components. After that, the connected components (part of an object) were labelled using the function '*bwboundaries*' in an ascendant order according to the number of connected regions.

The labelled objects with less than 80-pixel components were substituted by null values (or zeroes = 0's), in order to make them as part of the background pixels. This procedure allowed eliminating most of the noise points that still remained above the free surface, and the position of the air-water interface was then obtained, represented by the maximum positions of pixels with non-zero values in the vertical axis. Finally, the pixel coordinates were changed to spatial coordinates corresponding to the real scale. In order to verify the adequacy of the results, the final free surface profiles obtained were superimposed to the original frames, showing good agreement.
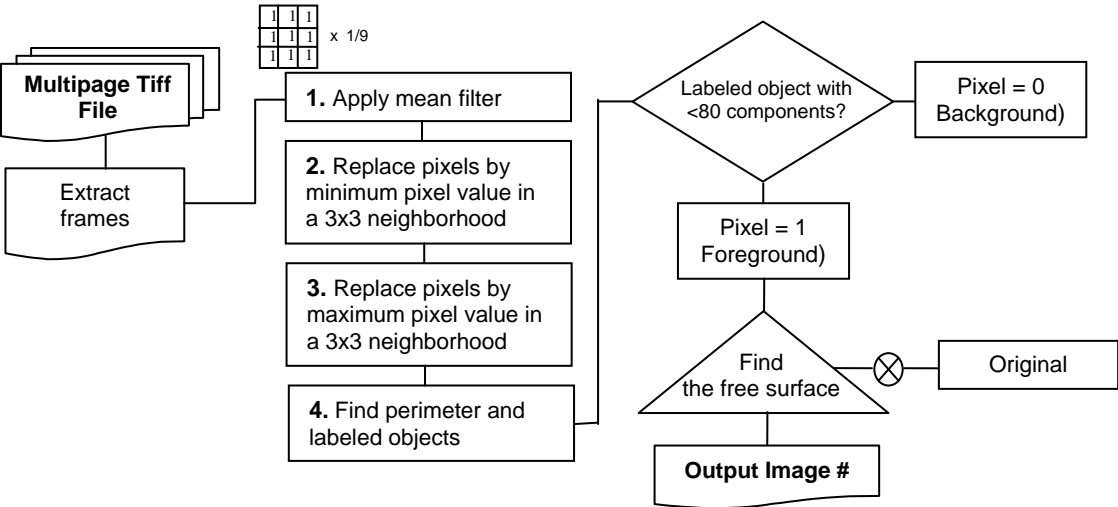

Figure 2 – Scheme of sequential steps used in image analysis.

2.2. Ultrasonic sensor

The ultrasonic sensor measures the distance from the sensor to the free surface, furnishing the instantaneous level of the flow. The measurements were carried out in the central line of the flume using the sensor GoMotion Vernier ®.The waves emitted by the sensor have a conic shape, with an angle of 15 to 20° in relation to the central line of the beam. The sensor was moved along the longitudinal distance in a displacement track, in order to obtain the free surface profile of the flow. The sampling time was 120 seconds for each position, horizontally distant 2 cm from each other. The sampling rate was 25 Hz.

The water droplets and the large slope of the free surface may cause eventual differences between the measured and the "real" depth of the water. If the free surface presents a large slope, the ultrasonic wave reflected by the surface may not reach the sensor beam, introducing outliers in the data set. A criteria based on box plot diagrams was used for removing the outliers. The procedures are described in detail in Simões *et al* (2010). Briefly, the data that exceeded the limits: $(qr_1 - 1.5 \cdot IQ)$ and $(qr_3 + 1.5 \cdot IQ)$ were disregarded for the calculation of the mean flow depths, in which qr_1 and qr_3 are the first and third interquartile respectively, and IQ is the difference between qr_3 and qr_1. Figure 3 sketches the mentioned procedure.
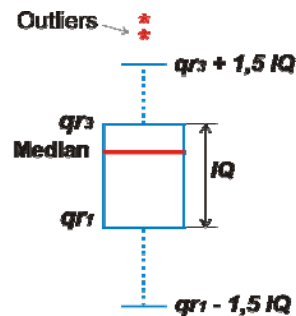

Figure 3 - Components of a box-plot.

3. EXPERIMENTAL RESULTS

3.1. Image analysis

Figure 5 shows the images resulted for each step of the described image processing, using one of the registered frames (frame #11). Figure 5h was then magnified to verify the superposition between the free surface determined by the computational runs (blue line) and the free surface observable in the original image, which is shown in Fig. 4. Even the small variations of the interface could be properly detected.

In some images, the final free surface line presented few discontinuities, with some calculated points located above or under the real interface. This happened at positions where the light intensity was attenuated close to the free surface, or in cases in which some noise remained above the interface. However, such events were limited to few images and few points in the images, not affecting the general good results of this method.
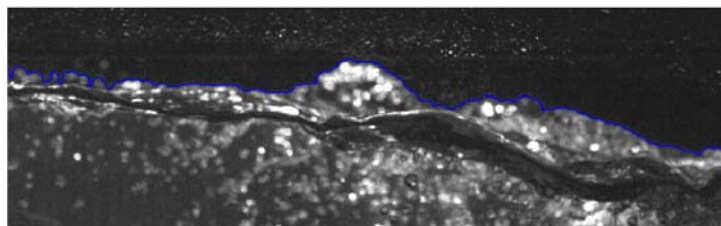

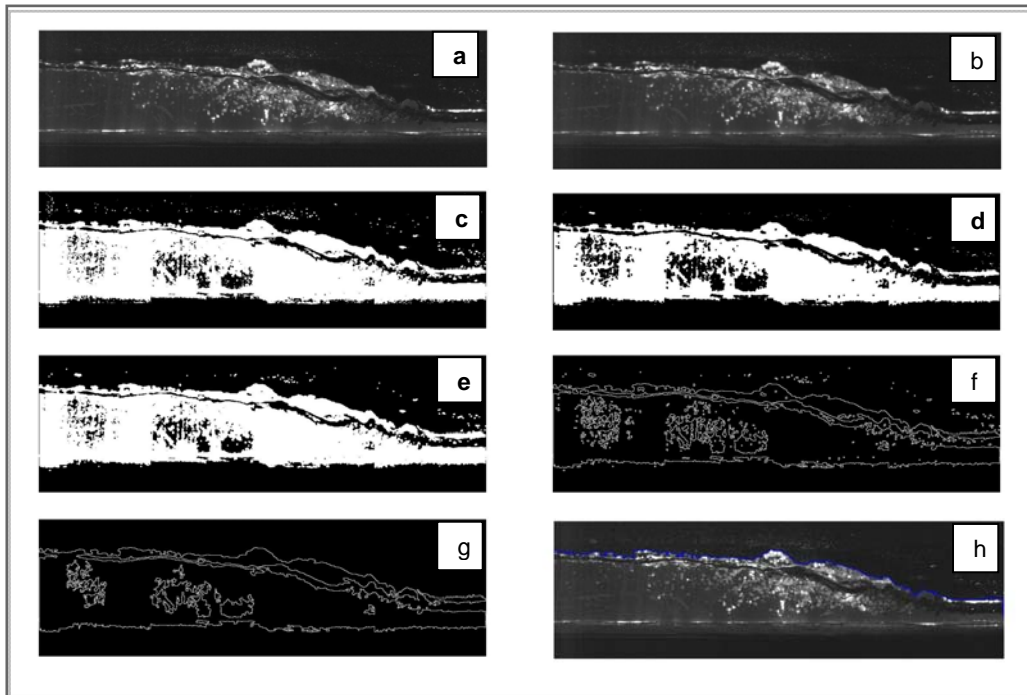Figure 4 – Detail of the interface. Zoomed area of the Figure 5 h.

Figure 5 – Sequential results of the processing: *a)* Cropped image #11 from the video; *b)* Media pixel intensity; *c)* Binary image; *d)* Minimum pixel intensity; *e)* Maximum pixel intensity; *f)* Perimeter and labelled objects; *g)* Exclusion of labelled objects with less than 80 pixel components; *h)* Final image.

3.2. Air-water interface

Figure 6 presents comparative plots of the mean free surface profiles obtained using the ultrasound sensor and the image analysis. The supercritical depth is imposed by the gate opening, which was fixed at 2.5 cm (y_1=2.7), while the subcritical depth is around 8.0 cm. The mean depth of the image analysis was based on the range of video frames #1 to #4000, corresponding to 20 seconds of video recording. Figure 6 includes the profile of Chachereau & Chanson (2011) for F_1 = 2.4 and the empirical profile of Hager (1993), which is dependent on L_r (roller length), x (longitudinal distance), y_1, and y_2. The value of L_r was calculated accordingly to the equation of Hager *et al* (1990), which was in accordance to the roller length observed in the present study. Although slight differences exist mainly in the roller region, the evolutions of the mean depths with the longitudinal axis are very similar. The profile obtained from the image analysis approximated very well the Hager (1993) formula.

Regarding the region of supercritical flow, as already mentioned, the depth is 2.7 cm. However, the depths obtained for this region using the ultrasonic sensor are slightly higher, probably because of the toe oscillation, affecting the values registered by the sensor. On the other hand, in the image analysis of this region, the depth is sometimes underestimated as a consequence of the low pixel intensity close to the gate.

In Figure 7, obtained evolutions of the free surface for each 5 seconds of record (1000 frames) are presented for the first 35 cm of the flow. It is possible to observe that the profiles do not change their general characteristic shape along time. The oscillation of the toe position is presented in Figure 8. The toe position was defined as the end of the horizontal supercritical surface. It was evaluated for each set of 100 images (total of 40 sets), based on visual analysis of the mean profiles. The maximum variation of the toe position was 4.5 cm for the time interval analysed here (Figure 8). The distances indicated in Figure 7 and Figure 8 refers to the length between the first pixel (considered as the zero position) and the jump toe.
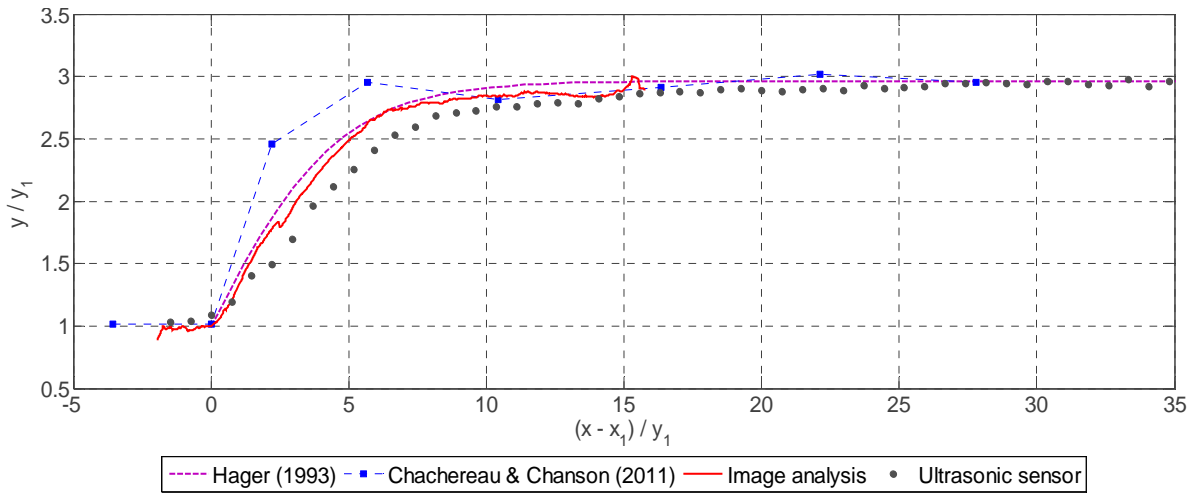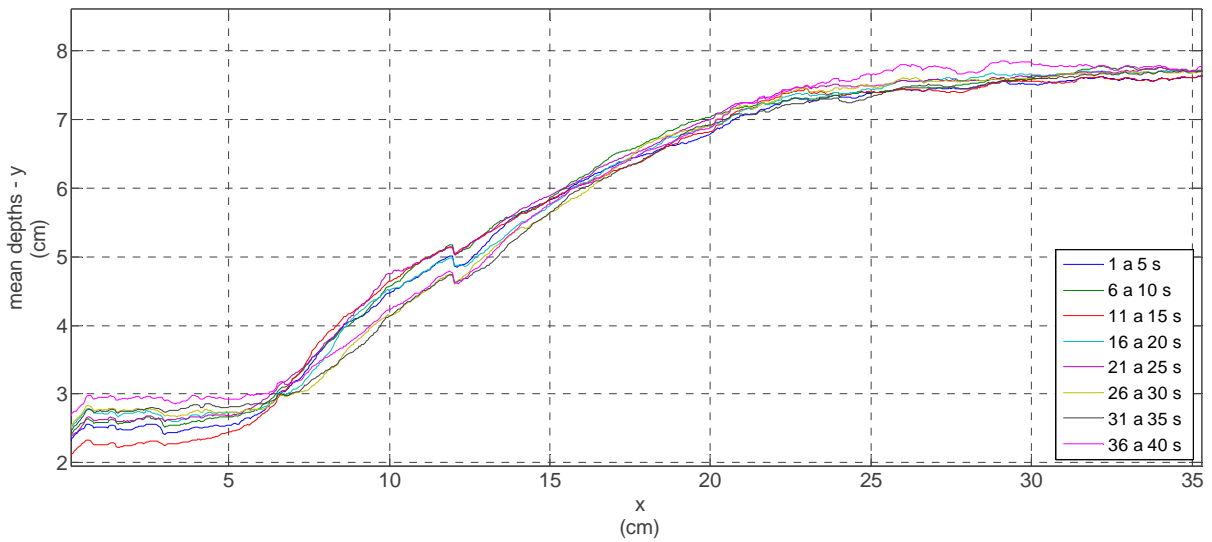
Figure 6 – Mean free surface profile.

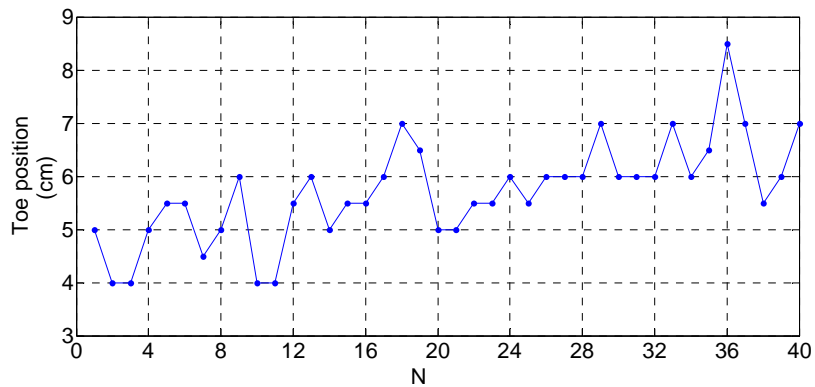Figure 7 - Time evolution of the mean free surface profile.

Figure 8 - Variation of toe position. N is the set of 100 images (40 sets).

In order to quantify a minimum sample time necessary to obtain stable results for the mean free surface profile, the root of the square differences (*RSD*) was calculated (Eq. 1). The decay curve of the obtained *RSD* values (Figure 9) shows that, after approximately 1900 frames, the RSD becomes inferior to 0.5. Therefore, 4.5 seconds is the minimum sample time needed to produce a mean free surface profile almost invariable in time.

$$RSD_i = \sum_{pixel=1}^{pixel=1024} \sqrt{\left(y_{profile,1:i} - y_{mean,profile}\right)^2}$$

(1)

where, RSD_i is root of the square differences for each frame i; $y_{profile,1:i}$ is the mean free surface profile using images 1 to i; $y_{mean,profile}$ is the mean free surface profile (in meters) calculated using 4000 images.
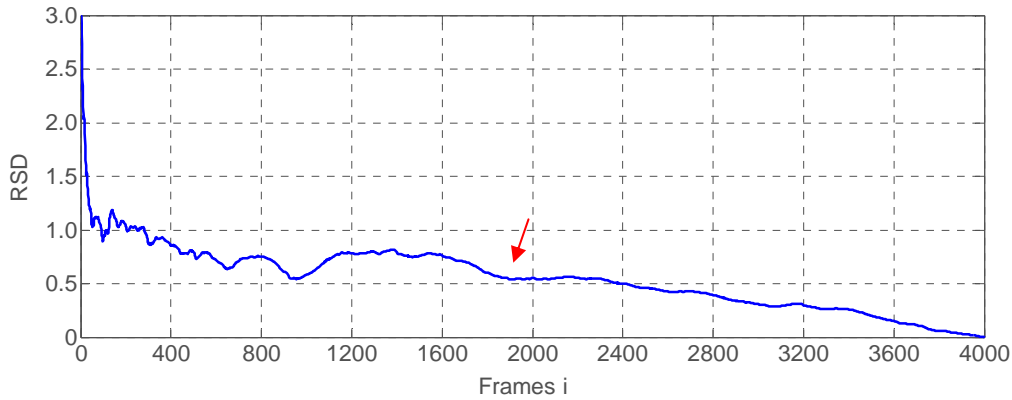

Figure 9 - RSD for i varying from 1 to 4000 frames.

Figure 5 was used to extract the profile of the interface through image analysis. Additionally, the internal distribution of bubbles, related to the structure of the roller region, may also be seen. Both flow characteristics (surface profile and roller structure) are related, but the structure of the roller is only visible through transparent walls experiments. Therefore, in practical channel conditions the roller structure must be evaluated based on alternative measurements, which leads to the convenience of Figure 6, which shows that ultrasound measurements superpose well to image analysis experiments. In this sense, the present study points to the convenience of use of the ultrasound sensor for practical experiments.

4. CONCLUSIONS

The profiles of the air-water interface of a hydraulic jump with $F_1=2.39$ was obtained through ultrasonic sensors and image processing techniques. Whereas the ultrasonic sensor furnishes punctual values, the image provides information of all the field of view. This characteristic of image analysis is interesting for the study of the flow structure in complex phenomena, like hydraulic jumps. On the other hand, the ultrasound method may be applied in practical channel flows, in order to obtain the surface profiles. The good superposition of the profiles obtained with both techniques confirms the adequacy of both methods for studying free surface features. Besides, it suggests the use of ultrasound sensors for practical measurements, associated to laboratory results of image analysis.

5. ACKNOWLEDGMENTS

6. REFERENCES

Bung, D.B. (2011), *Non-intrusive measuring of air-water flow properties in self-aerated stepped spillway flow*, Proc. 34th IAHR World Congress, Brisbane, Australia, 26 June-1 July, Engineers Australia Publication, Eric Valentine, Colin Apelt, James Ball, Hubert Chanson, Ron Cox, Rob Ettema, George Kuczera, Martin Lambert, Bruce Melville and Jane Sargison Editors, pp. 2380-2387.

Bung, D.B. (2013), *Non-intrusive detection of air-water surface roughnes in self-aerated chute flows*, Journal of Hydraulic Research, 51 (3), 322-329.

Chachereau, Y. and Chanson, H. (2010), *Free-surface turbulent fluctuations and air-water flow measurements in hydraulic jumps with small Froude numbers*. Report CH78/10, The University of Queensland, Brisbane.

Chachereau, Y. and Chanson, H. (2011), *Free-surface fluctuations and turbulence in hydraulic jumps*, Experimental Thermal and Fluid Science, 35 (6), 896-909.

Chanson, H. (2009), *Current knowledge in hydraulic jumps and related phenomena. A survey of experimental results*, European Journal of Mechanics B/ Fluids, 28, 191-210.

Hager, W.H., Bremen, R. and Kawagoshi, N. (1990), *Classical hydraulic jump: length of roller,* Journal of Hydraulic Research, 28 (5), 591-608.

Hager, W.H. (1993), *Classical hydraulic jump: free surface profile*, Canadian Journal of Civil Engineering, 20, 536-539.

Kucukali, S. and Chanson, H. (2008), *Turbulence measurements in the bubbly flow region of hydraulic* jumps, Experimental Thermal and Fluid Science, 33, 41-53.

Leandro, J., Carvalho, R., Chachereau, Y. and Chanson, H. (2012), *Estimating void fraction in a hydraulic jump by measurements of pixel intensity*, Experiments in Fluids, 52 (5), 1307-1318.

Lima, A.C.M. (2004), *Determination of turbulent structures of aerated flows in chutes using PIV*. Thesis, University of São Paulo, Sao Carlos, Brazil. [in Portuguese].

Lima, A.C.M., Schulz, H.E., Gulliver, J.S., Ling, J.T. and Ling, R.S. (2008), *Air uptake along the lower nappe of a spillway aerator,* Journal of Hydraulic Research, 46 (6), 839-843.

Lima, A.C.M., Schulz, H.E. and Gulliver, J.S. (2009), *Air uptake along the lower nappe of a spillway aerator (Discussion of Falvey, H.T.)*, Journal of Hydraulic Research, 47, 683-684.

Lin, C., Hsieh, S., Lin, I., Chang, K. and Raikar, R.V. (2012), *Flow property and self-similarity in steady hydraulic jumps*, Experimental Fluids, 53, 1591-1616.

Long, D., Rajaratnam, N., Steffler, P.M. and Smy, P.R. (1991), *Structure of flow in hydraulic jumps*, Journal of Hydraulic Research, 29 (2), 207-218.

Misra, S.K., Thomas, M., Kambhamettu, C., Kirby, J.T., Veron, F. and Brocchini, M. (2006), *Estimation of complex air-water interfaces from particle image velocimetry images*, Exp. in Fluids, 40, 764-775.

Misra, S.K., Kirby, J.T., Brocchini, M., Veron, F., Thomas, M. and Kambhamettu, C. (2008), *The mean and turbulent flow structure of a weak hydraulic jump*, Physics of Fluids, 20, 035106.

Murzyn, F., Mouazé, D. and Chaplin, J.R. (2007), *Air-water interface dynamic and free surface features in hydraulic jumps*, Journal of Hydraulic Research, 45 (5), 679-685.

Murzyn, F. and Chanson, H. (2009a), *Free-surface fluctuations in hydraulic jumps: Experimental observations*, Experimental Thermal and Fluid Science, 33, 1055-1064.

Murzyn, F. and Chanson, H. (2009b), *Non intrusive measurement technique for dynamic free-surface characteristics in hydraulic jumps*, in 33rd IAHR Biennial Congress: Water Engineering for a Sustainable Environment, Vancouver, British.

Rajaratnam, N. (1995), *Almanac of energy dissipation mechanisms,* in Vischer, D.L. and Hager, W.L., Energy Dissipators, A.A. Balkema, Rotterdam, pp. 23-42.

Rodríguez-Rodríguez, J., Marugán-Cruz, C., Aliseda, A. and Lasheras, J.C. (2011), *Dynamics of large turbulent structures in a steady breaker*, Experimental Thermal and Fluid Science, 35, 301-310.

Simões, A.L.A., Schulz, H.E. and Porto, R.M. (2010), *Simulação numérica e verificação experimental da posição da superfície livre de um ressalto hidráulico em um canal retangular*. Paper presented to XXIV Congresso Latinoamericano de Hidráulica, Punta del Este, Uruguay. [in Portuguese].

Simões, A.L.A., Schulz, H.E. and Porto, R.M. (2011a), *Stepped and smooth spillways: resistance effects on stilling basin lengths (Discussion of Takahashi, M. and Ohtsu, I.)*, Journal of Hydraulic Research, 49 (3), 404-408.

Simões, A.L.A., Schulz, H.E. and Porto, R.M. (2011b), *Transition length between water and air-water flows on stepped chutes*, in Preprints of the 6th International Conference on Computational and Experimental Methods in Multiphase and Complex Flow, Kos, Greece, June 15-17, 2011, pp. 95-105.

Simões, A.L.A., Schulz, H.E., Porto, R.M. and Gulliver, J.S. (2013), *Free-surface profiles and turbulence characteristics in skimming flows along stepped chutes*, Journal of Water Resource and Hydraulic Engineering, 2, 1-12.